Electronic Supplementary Material (ESI) for Environmental Science: Nano.

Supplementary Information

Natural organic matter facilitates formation and microbial methylation of mercury selenide nanoparticles

Qing Chang[1#], Zhanhua Zhang[1#], Yunyun Ji[1], Li Tian[1], Wei Chen[1], Tong Zhang[1*]

[1] *College of Environmental Science and Engineering, Ministry of Education Key Laboratory of Pollution Processes and Environmental Criteria, Tianjin Key Laboratory of Environmental Remediation and Pollution Control, Nankai University, Tianjin 300350, P. R. China*

* Corresponding author: Tel (Fax): +86 22-66229516; E-mail: zhangtong@nankai.edu.cn.

# These authors contributed equally to this work.

Table S1. Physicochemical properties of the reaction products of inorganic divalent mercury (Hg) and selenium (Se) in the presence of natural organic matter (NOM).

NOM	Aging time (d)	Geometric diameter (nm) [1]	Geometric specific surface area (m^2 g^{-1}) [2]	Hydrodynamic diameter (nm) [3]
Suwannee River fulvic acid (SRFA)	1	4.35 ± 0.64 *b*	167 ± 34.6 *a*	179 ± 17 *c*
	8	5.32 ± 0.52 *b*	139 ± 29.8 *ab*	196 ± 16 *bc*
	15	5.35 ± 0.61 *b*	136 ± 32.1 *ab*	244 ± 20 *b*
Suwannee River humic acid (SRHA)	1	6.90 ± 0.81 *a*	106 ± 37.3 *b*	346 ± 26 *a*
	8	6.88 ± 0.42 *a*	106 ± 21.8 *b*	355 ± 22 *a*
	15	7.02 ± 0.72 *a*	104 ± 35.1 *b*	382 ± 50 *a*

[1] Geometric diameters are estimated from individual monomers observed in transmission electron microscopy (TEM) images (Figure 1). Data represent mean ± 1 standard deviation of 100 particles. Statistically different values ($p < 0.05$) are indicated by italic lowercase letters according to the one-way analysis of variance (ANOVA).

[2] Geometric surface areas are calculated assuming spherical particles with a density of 8.24 g cm^{-3} (Institute of Experimental Mineralogy, Russian Academy of Science. Crystallographic and Crystallochemical Database for Minerals and their Structural Analogues. http://database.iem.ac.ru/mincryst/index.php). Data represent mean ± 1 standard deviation of 100 particles. Statistically different values ($p < 0.05$) are indicated by italic lowercase letters according to the one-way ANOVA.

[3] Hydrodynamic diameters are measured using dynamic light scattering. Data represent mean ± 1 standard deviation of triplicate samples. Statistically different values ($p < 0.05$) are indicated by italic lowercase letters according to the one-way ANOVA.

Table S2. X-ray photoelectron spectroscopy (XPS) spectral features of Hg 4f signals for the reaction products of inorganic divalent Hg and Se in the absence and presence of SRFA or SRHA, and of C 1s signals for the reaction products of inorganic divalent Hg and Se in the presence of SRFA or SRHA.

Sample	Signal	Assigned peak	Binding energy (eV)
HgSe	Hg 4f	Hg $4f_{5/2}$	104.5
		Hg $4f_{7/2}$	100.4
SRFA–HgSe	C 1s [1]	C–C, C=C	284.8
		C–O, C–O–C	286.6
		O=C–O	288.9
	Hg 4f	Hg $4f_{5/2}$	104.1
		Hg $4f_{7/2}$	100.1
SRHA–HgSe	C 1s [1]	C–C, C=C	284.8
		C–O, C–O–C	286.5
		O=C–O	288.6
	Hg 4f	Hg $4f_{5/2}$	104.3
		Hg $4f_{7/2}$	100.2

[1] The binding energy values of the C 1s peaks corresponding to the aromatic rings (C–C, C=C), hydroxyl/epoxy groups (C–O, C–O–C) and carboxyl groups (O=C–O) of uncomplexed NOM are 284.8, 286.5 and 288.5 eV, respectively.[1-4]

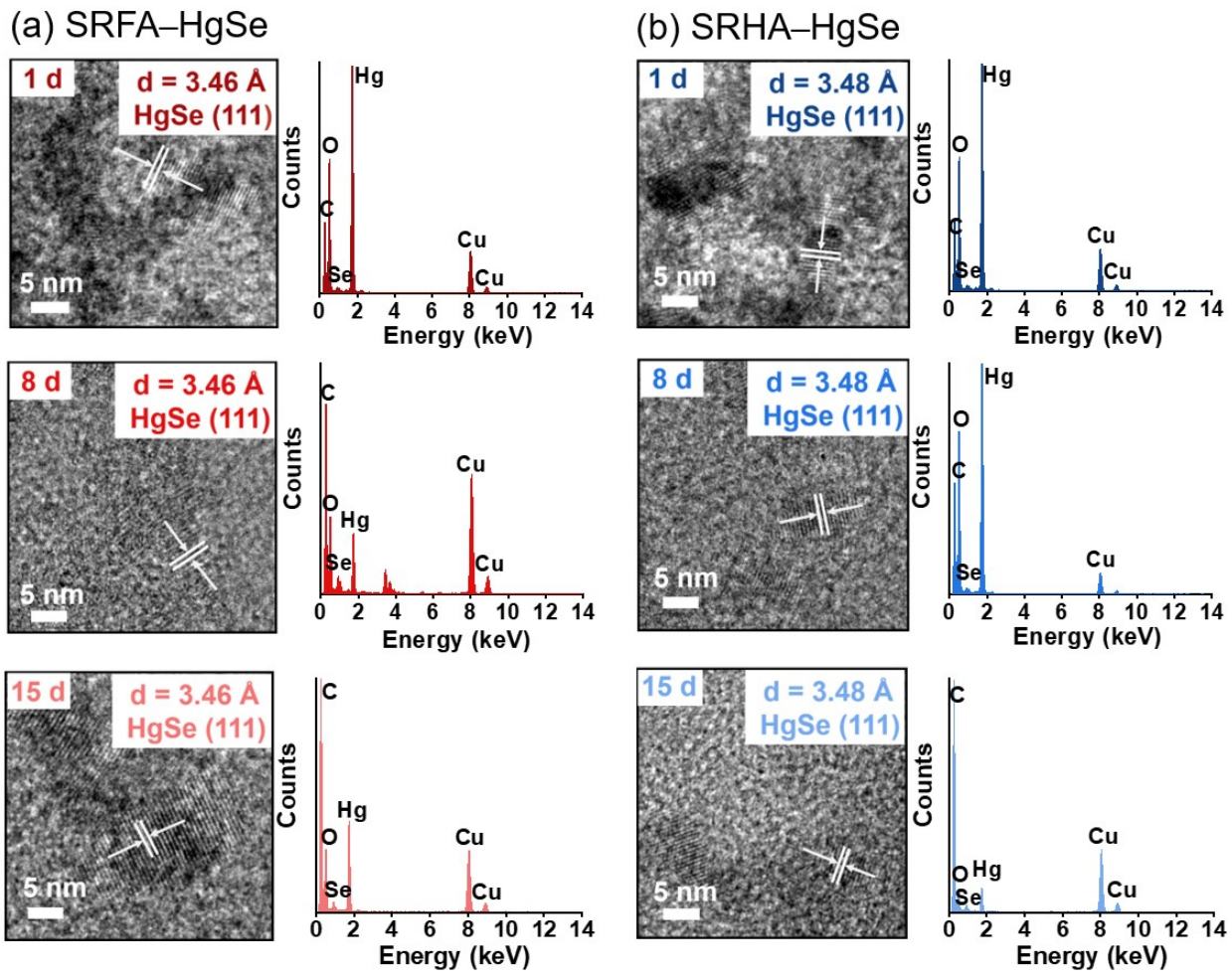

Fig. S1. High-resolution transmission electron microscopy (HR-TEM) images and energy dispersive X-ray spectroscopy (EDX) spectra of the reaction products of inorganic divalent Hg and Se in the presence of SRFA (a) or SRHA (b) aged for 1 d, 8 d and 15 d.

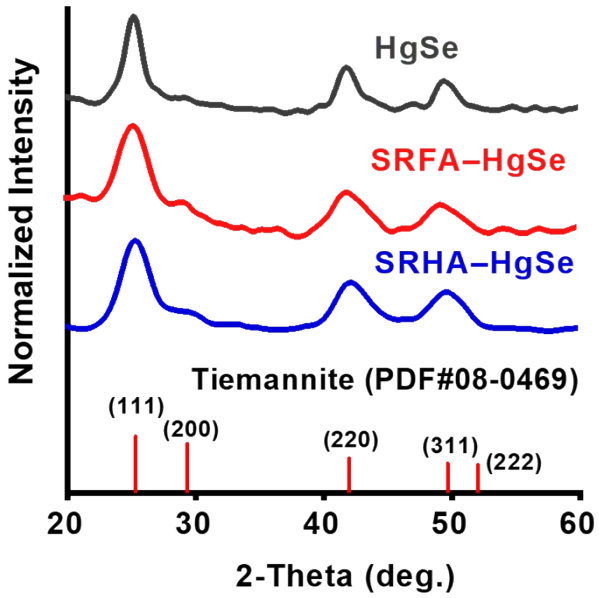

Fig. S2. X-ray diffraction (XRD) spectra of the reaction products of inorganic divalent Hg and Se in the absence and presence of SRFA or SRHA.

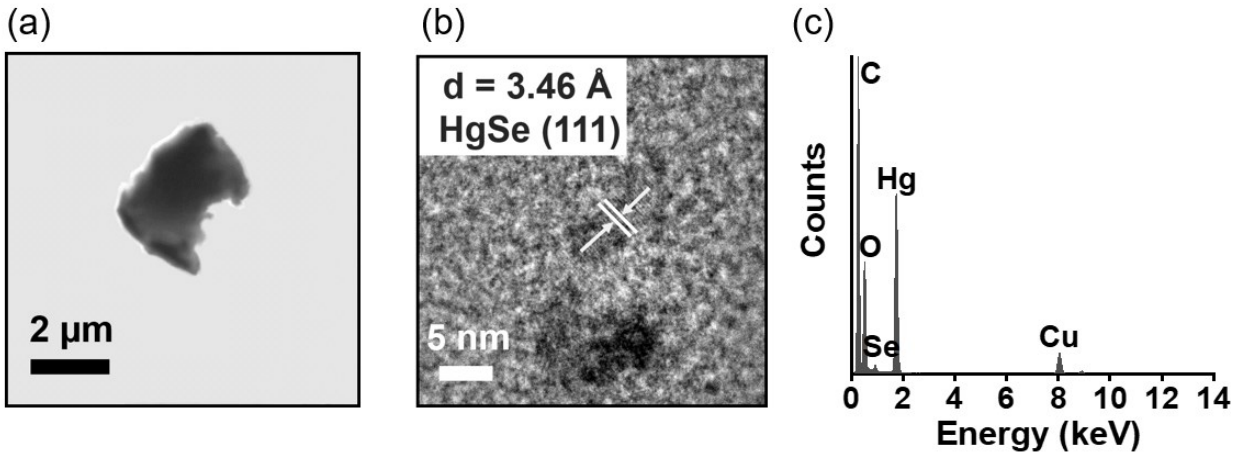

Fig. S3. TEM image (a), HR-TEM image (b) and EDX spectrum (c) of the reaction products of inorganic divalent Hg and Se in the absence of NOM.

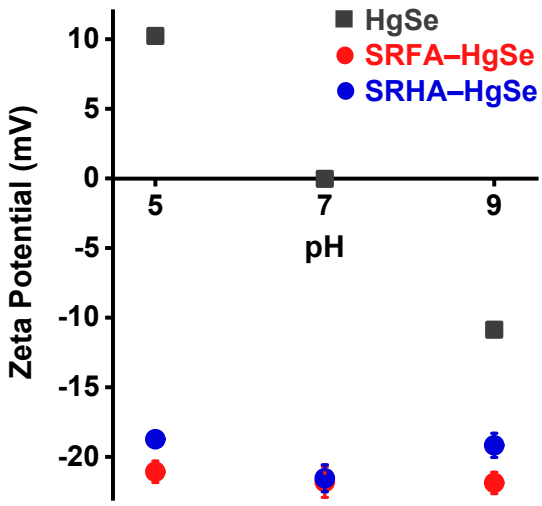

Fig. S4. Zeta potential measurements of the reaction products of inorganic divalent Hg and Se in the absence and presence of SRFA or SRHA at different pH conditions. Error bars represent ± 1 standard deviation of replicate samples (n = 3).

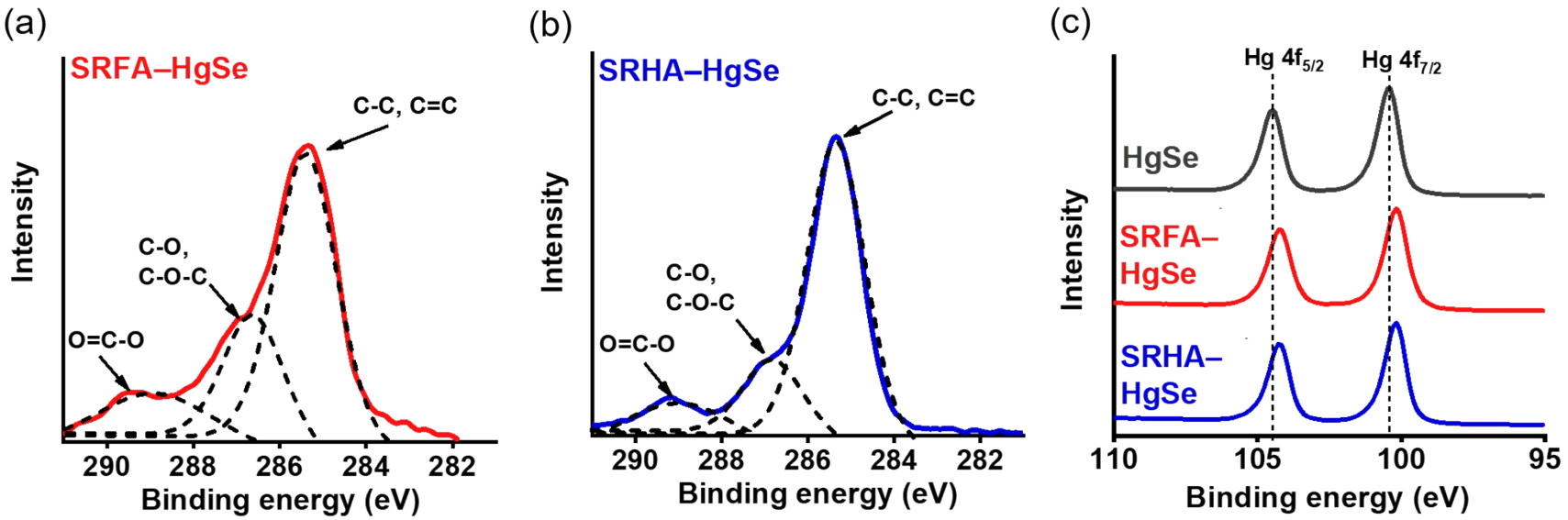

Fig. S5. XPS spectra of C 1s signals of the reaction products of inorganic divalent Hg and Se in the presence of SRFA (a) or SRHA (b). XPS spectra of Hg 4f signals (c) of the reaction products of inorganic divalent Hg and Se in the absence and presence of SRFA or SRHA.

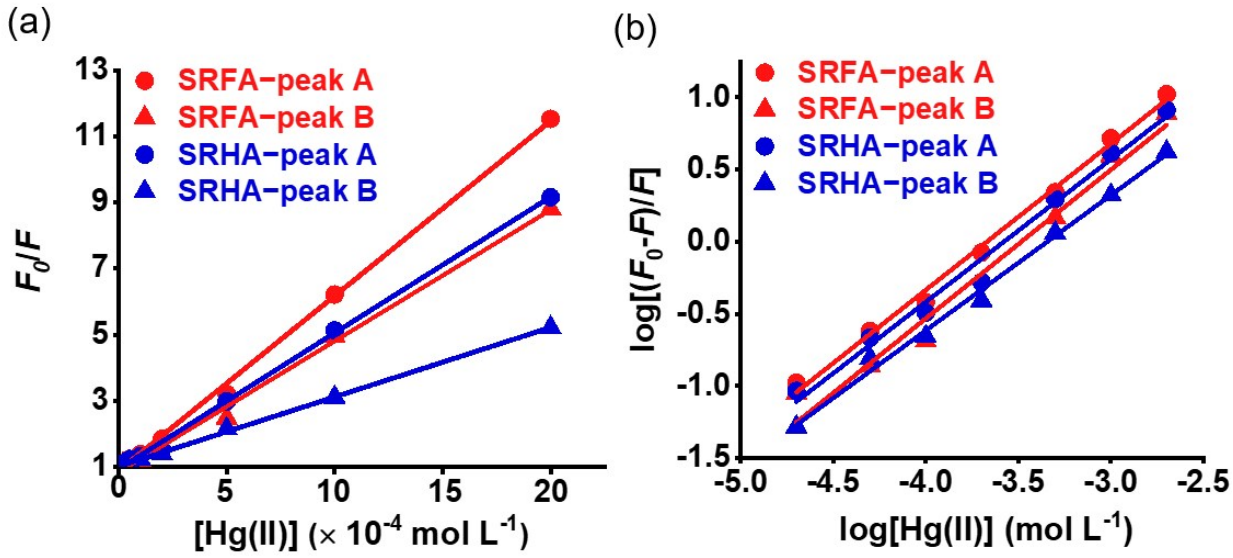

Fig. S6. Stern–Volmer plot (a) and static quenching data fitting (b) for fluorescence quenching of peak A and peak B of SRFA or SRHA. The solid lines represent the linear regression fitting of fluorescence data.

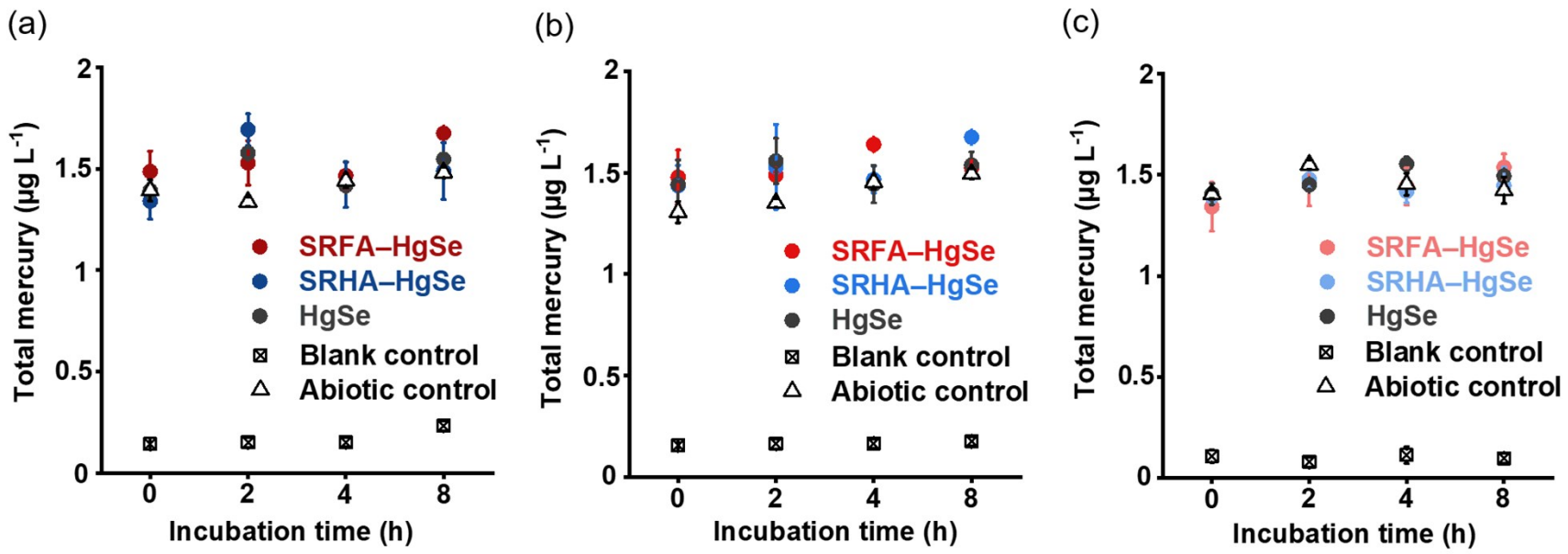

Fig. S7. Total mercury concentration measured from *Desulfovibrio desulfuricans* ND132 cultures after exposure to the reaction products of inorganic divalent Hg and Se in the absence and presence of SRFA or SRHA aged for 1 d (a), 8 d (b) and 15 d (c). Blank control represents active cultures with no mercury addition. Abiotic control represents un-inoculated media spiked with the same amount of $Hg(NO_3)_2$. Error bars represent ± 1 standard deviation of replicate samples (n = 3).

Reference

1. Y. Wang, K. Yang and D. Lin, Nanoparticulate zero valent iron interaction with dissolved organic matter impacts iron transformation and organic carbon stability, *Environ. Sci.: Nano*, 2020, **6**, 1818–1830.

2. P. L. Desbene, L. Silly, J. P. Morizur and M. Delamar, XPS analysis of humic and fuvic acid, *Anal. Lett.* 1986, **19**, 2131−2140.

3. J. R. Araujo, B. S. Archanjo, K. R. de Souza, W. Kwapinski, N. P. S. Falcão, E. H. Novotny and C. A. Achete, Selective extraction of humic acids from an anthropogenic Amazonian dark earth and from a chemically oxidized charcoal, *Biol. Fertil. Soils*, 2014, **50**, 1223−1232.

4. L. Wei, T. Hong, K. Cui, T. Chen, Y. Zhou, Y. Zhao, Y. Yin, J. Wang and Q. Zhang, Probing the effect of humic acid on the nucleation and growth kinetics of struvite by constant composition technique, *Chem. Eng. J.*, 2019, **378**, 122130.